



EUROfusion

WPPFC-CPR(18) 21128

M Houry et al.

**The very high spatial resolution infrared
thermography on ITER-like tungsten
monoblocs in WEST Tokamak**

Preprint of Paper to be submitted for publication in Proceeding of
30th Symposium on Fusion Technology (SOFT)



This work has been carried out within the framework of the EUROfusion Consortium and has received funding from the Euratom research and training programme 2014-2018 under grant agreement No 633053. The views and opinions expressed herein do not necessarily reflect those of the European Commission.

This document is intended for publication in the open literature. It is made available on the clear understanding that it may not be further circulated and extracts or references may not be published prior to publication of the original when applicable, or without the consent of the Publications Officer, EUROfusion Programme Management Unit, Culham Science Centre, Abingdon, Oxon, OX14 3DB, UK or e-mail Publications.Officer@euro-fusion.org

Enquiries about Copyright and reproduction should be addressed to the Publications Officer, EUROfusion Programme Management Unit, Culham Science Centre, Abingdon, Oxon, OX14 3DB, UK or e-mail Publications.Officer@euro-fusion.org

The contents of this preprint and all other EUROfusion Preprints, Reports and Conference Papers are available to view online free at <http://www.euro-fusionscipub.org>. This site has full search facilities and e-mail alert options. In the JET specific papers the diagrams contained within the PDFs on this site are hyperlinked

The very high spatial resolution infrared thermography on ITER-like tungsten monoblocs in WEST Tokamak

M. Houry^a, C. Pocheau^a, M-H. Aumeunier^a, C. Balorin^a, K. Blanckaert^a, Y. Corre^a, X. Courtois^a, F. Ferlay^a, J. Gaspar^b, S. Gazzotti^a, A. Grosjean^a, Th. Loarer^a, H. Roche^a, A. Saille^a, S. Vives^a and the WEST Team

^a CEA-IRFM, F-13108 Saint-Paul-Lez-Durance, France

^b Aix-Marseille Université, CNRS, IUSTI UMR 7343, 13013 Marseille, France

A new Infrared diagnostic has been developed by CEA-IRFM and installed in the WEST tokamak to measure surface temperature of the actively cooled W-monoblocs components as foreseen for the ITER Divertor units, with a very high spatial resolution of 100 μ m. The goals are to investigate the effects of the shaping of these components on the heat load deposition pattern, the evolution of pre-damaged components specifically introduced in WEST, the behavior of the leading edges regarding the assembling tolerances between adjacent monoblocs, and finally to contribute to the specification assessment of the ITER divertor units. In WEST, each Plasma Facing Unit is composed of 35 W-monoblocs of individual surface of 28x12mm. To analyze heat load pattern and phenomena on such tiny surfaces, the leading edges and in the narrow gaps between monoblocs (400-500 μ m), a 100 μ m spatial resolution is required. Then, a Very High spatial Resolution (VHR) infrared diagnostic has been specially developed at CEA-IRFM. The VHR operates at 1.7 μ m wavelength to take advantage of the dynamic of the signal for the temperature range (400 to 3600°C). The VHR infrared diagnostic is now operational above the divertor sector made of actively cooled W-monoblocs and graphite inertial components with W coating. This paper gives a description of the diagnostic.

Keywords: ITER, Plasma facing components Protection, Diagnostics, infrared, tungsten monoblocs.

1. Introduction and context

The ITER full tungsten (W) divertor will be made of several hundred thousand individual W monoblocs with exposed surface of few cm². Assembled on a pipe like a rosary for the cooling by a water loop, the requirement for the mechanical assembly tolerance is highly demanding [1]. Indeed, due to the low angle of incidence of the magnetic field lines, on the surface of the components, to spread the heat loads, a misalignment of the components can induce a particle impact on the side of the component close to perpendicular (Fig. 1) [2].

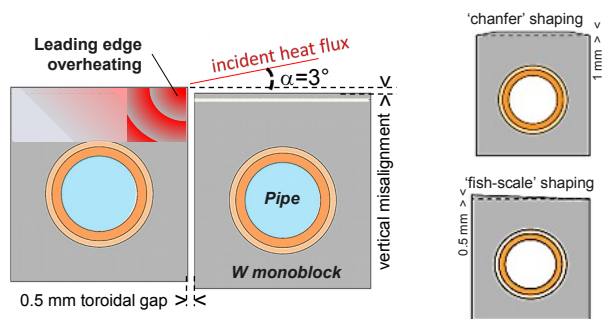


Fig. 1: Cross section of the ITER-like Plasma facing Unit, showing shaping and effect of vertical misalignment.

The heat loads deposited per unit of area can then lead to a local melting of components and irreversible damages [3], [4]. Designs are proposed to reduce the

risk induced by misalignments. They consist of a machining of component surface for a shading effect over the successive components or a chamfer on the edges of the components (“fish-scale” shaping, Fig. 1) or a chamfer on the edges of the components (“chamfer shaping, Fig. 1). The misalignment tolerance for the components assembly and the capability of the applied designs to reduce the risk of damage, as well as the impact of damages on the heat exhaust capacity of the components are crucial issues for ITER [5].

With the modification of the Tore Supra tokamak into WEST, the CEA-IRFM offers a platform to test the concept and designs of the Plasma Facing unit (PFU) made of Tungsten monoblocs for ITER [6], [7]. PFUs of different manufacturers and different design and shaping will thus be tested under different plasma conditions and with ITER-relevant heat loads deposition ranging from 10MW/m² in steady state up to 20MW/m² of transient peak heat flux.

The observation of phenomena related to heat loads on the leading edges of the components is a challenge. Indeed, phenomena occur on very narrow surfaces and with tricky angles and distances for observation purposes. Then, a Very High spatial Resolution (VHR) infrared diagnostic has been specially developed at CEA-IRFM to observe heat loads on ITER-like PFU.

2. Description of the diagnostic

2.1 Tokamak environment

The WEST divertor with the ITER-like PFUs is a conical surface at the bottom of the vacuum vessel. The observation on the divertor is made from an upper port. The line of sight between the first mirror and the divertor is about 2m, with an incidence close to 90° (Fig).

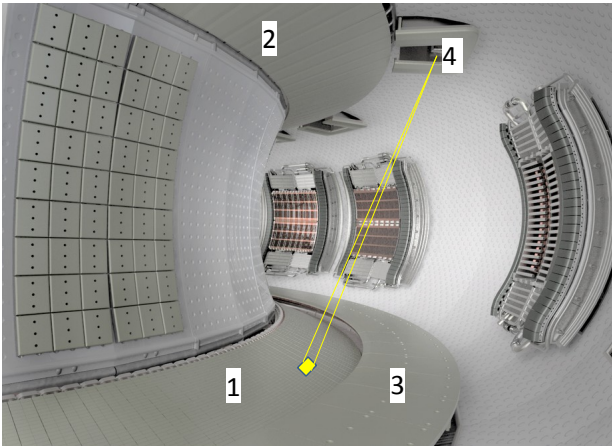


Fig 2: CAD view of the WEST Vessel. (1) lower divertor (2) upper divertor, (3) Baffle, (4) upper port with VHR diagnostic.

The head of the endoscope and the first mirror are positioned 30cm backward in the port to prevent the heat load deposition from particles and radiative flux. Thus, it was not necessary to install a water cooling system on the head of the endoscope, significantly reducing the design and integration constraints.

2.2 Optical design

The gaps between the monoblocs (0.5 to 1mm), the chamfers (1mm range) and the misalignments (maximum of 0.3mm) led to a requirement for the spatial resolution of 100µm; providing enough measurement points for analysis.

The observation of the components with a pixel resolution of 0.1mm constrains the objects and image fields of the optical design. The observed field is 64mm x 51mm with a matrix of 640x512 pixels with a pitch of 15µm, thus defining a transverse magnification of 6.67.

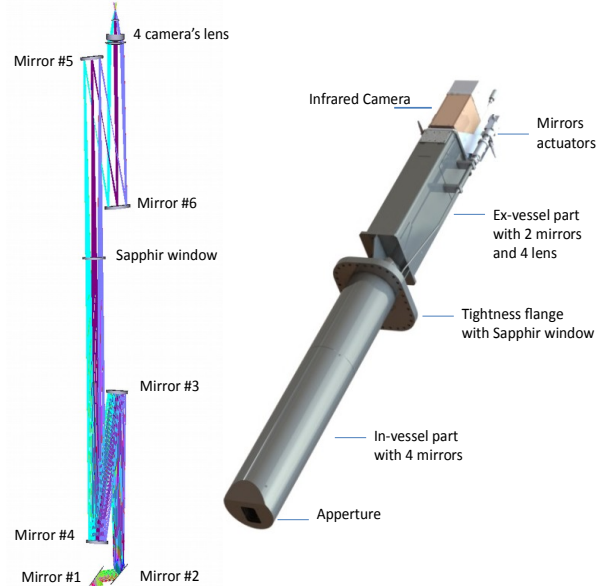


Fig 3: Design of the optical path (left part) CAD view of the VHR diagnostic (right part).

To achieve this high spatial resolution, the design of the VHR is made of 6 mirrors and 4 lenses (Fig 3) : 1 spherical mirror (#3), a cylindrical mirror (#4), 4 lenses and 4 flat mirrors (#1, #2, #5, #6); the first 2 can be remotely moved to scan the observable surface.

2.3 Mechanical design

The conceptual mechanical design of the endoscope is inspired by space industry. The endoscope structure is light, compact and “flexible-stiff” to sustain transient events such as disruptions. Modal vibrational frequency calculations have been performed to ensure that, in the vibratory environment of the tokamak, the structure of the endoscope could not resonate. Thus, this design does not present vibratory mode below 50Hz. The part under vacuum consists of successive platforms for the installation of mirrors, connected by tie rods and flexible structures. A stainless steel cylinder cover encloses the assembly without thermal contact with the internal structure (Fig 3 and 4). The dimension of the endoscope from one end to the other is 2.33m; the diameter of the in-vessel part is 200mm

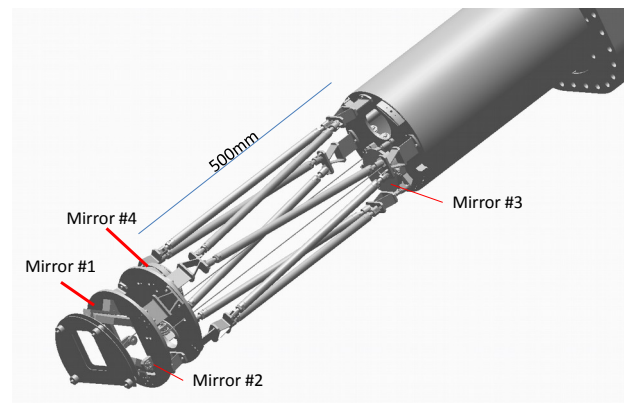


Fig 4: Design of the mechanical structure holding the mirrors (in-vessel part of the endoscope).

Due to the ripple effect and the displacement of the strike points on the divertor, the field of view, which is quite narrow (64*51mm), must be able to scan the divertor surface to reach the areas of interest. The two head mirrors are thus actuated to rotate on their axis of rotation (poloidal for the mirror 1 and toroidal for the mirror 2). The field of view can thus move on the divertor on a surface of 360x420mm, covering 14 PFUs (toroidal direction) and 28 monoblocs (poloidal direction). The actuators are located at the upper end of the endoscope (away from the magnetic field) and operate cables for the movement of the mirrors (Fig 3). The displacement of the field of view on the selected monoblocs is automated using a dedicated software.

Due to the conical shape of the divertor, the line of sight distance varies according to the observed field of view (± 4 cm). This is optically compensated by a motorized camera lens which allows adjusting the focus according to the observed area on the divertor.

2.4 Infrared camera

The infrared camera of the VHR is one of the 12 homemade WEST infrared cameras (Fig. 5) developed for the real time monitoring and protection of WEST components [8].

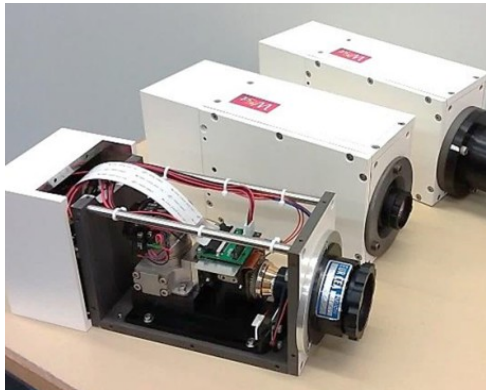


Fig 5: WEST Home-made cameras with soft iron magnetic shield.

The sensor is an InSb array which operate in the spectral range [1.5 - 5.0 μ m], with a pixel frame of 640x512 at 250Hz acquisition frame rate. A soft iron magnetic shielding surrounds the camera components against the magnetic fields of the tokamak. An actively cooled plate is fixed with screws on the casing to maintain a stable temperature. The band-pass filter installed few mm in front of the sensor is also cooled using a Peltier module to reduce the contribution of the background.

The bad pixels replacement, the correction of non-uniformity of the detector and the digital level to temperature conversion is performed in real time in an external FPGA board.

3. Performances

3.1 Temperature Measurement

Temperature calibration has been performed on CEA-IRFM test benches with a black body up to 1600°C with a point source and 500°C with an extended source. The extrapolation to temperature up to 3000°C has been achieved thanks to the good linearity of the sensor. Optical transmission of the endoscope has been measured at 55%. Emissivity remains a delicate point for absolute temperature measurement with metallic components. We use emissivity values from measurements performed on a dedicated test bed. Tungsten emissivity has been measured versus surface temperature, wavelength and surface state of the monoblocs (mainly its roughness). In addition, sensors embedded in the components of the divertor (thermocouples and Fiber Bragg Grating) contribute by cross-measurement to an optimization of the uncertainty on the emissivity and the surface temperature. The choice of the 1.7 μ m wavelength for the optimization of the measurement also offers an improvement on the absolute error on the temperature (compare to middle wavelength range). The choice of this wavelength is based on the very large temperature range (400 to 3600°C) foreseen for the experimental studies (up to melting of the leading edges).

3.2 Image Resolution

The modulation transfer function (MTF) is a basic performance measure of an imaging system describing the optical response of the system as a function of the spatial frequencies. The experimental MTF is found by using a slit-method. This technique is performed by imaging a thin slit (25 μ m) slightly tilted. The Figure 6 shows the measured MTF and a comparison with the pixel MTF (with a pixel of 0.1 mm in object plane). The response of our system is here limited by the optics (mainly by the diffraction phenomenon). We note that at 300 μ m, the MTF is 35% which is a commonly used lowest value for imaging contrast acceptance. Fig 6 (bottom) shows the slit response function (SRF) obtained by measuring the luminance ratio at a given (thin) slit width with a very wide slit width. At 100 μ m the SRF is 35% leading to an uncertainty of temperature of 15% at 1000°C [9].

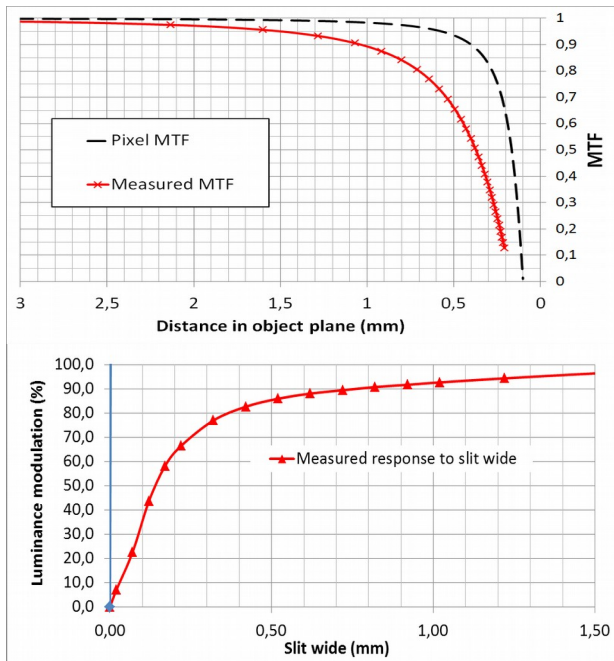


Fig 6: Modulation transfer function (upper figure) and Slit response function (bottom figure) of the VHR diagnostic.

3.3. Observation on WEST components

During previous WEST ramp-up campaigns, the heat loads were not sufficient to reach the temperature threshold of the VHR. However, images have been collected during events producing a lot of radiation such as disruption. The figure 7 is an image obtained during a disruption (pulse #52205); we clearly see the monoblocs of 2 ITER-like PFUs and on the right side an inertial PFU with W coating. The gaps and chamfer are clearly observed around the surfaces of the monoblocs.

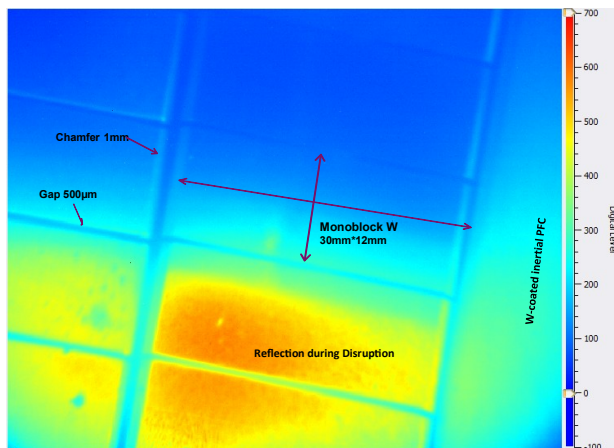


Fig 7: Image of the surface of the Plasma Facing Unit on lower Divertor during disruption.

4. Conclusion

The VHR infrared diagnostic on WEST is dedicated to observation of heat loads deposits on ITER-like PFUs. It offers a spatial resolution of $100\mu\text{m}$ (MTF at 35%), measuring temperature from 400°C with an accuracy close 15% at 1000°C .

The diagnostic is operational and follows the ramp-up of WEST, ready for observation of heat loads on leading edges and effects from misalignments and components surface shaping.

Already some improvements are being studied. They concern (i) the implementation of a two-color measurement for a better accuracy on the measurement of temperature and (ii) fast measurement for the observation of fast thermal transient events such as the ELM energy deposition.

Acknowledgments

“This work has been carried out within the framework of EUROfusion Consortium and has received funding from Euratom research and training programme. The views and opinions expressed herein do not necessarily reflect those of the European Commission.

References

- [1] S. Carpentier *et al.*, 2014 *Phys. Scr.* T159 014002
- [2] Y. Corre, *et al.*, *Nucl. Fusion* 57 (2017) 016009.
- [3] J.P. Gunn *et al.*, *Nucl. Fusion* 57 (2017) 046025
- [4] R. Dejarnac *et al.*, *Nucl. Fusion* 58 (2018) 066003
- [5] R.A.Pitts *et al.*, *Journal of Nuclear Materials*, volume 438, 2013, S48
- [6] J. Bucalossi, *et al.* *Fusion Eng. Des.* **89** (2014) 907–912.
- [7] D. Guilhem, *et al.*, *Phys. Scr.* 167 (2016) 014066.
- [8] X. Courtois *et al.*, this conference Proc.
- [9] X. Courtois *et al.* *Fusion Eng. Des.* In Press, doi 10.1016/j.fusengdes.2018.05.042